Using Patient-Specific Induced Pluripotent Stem Cells and Wild-Type Mice to Develop a Gene Augmentation-Based Strategy to Treat *CLN3*-Associated Retinal Degeneration

Luke A. Wiley, Erin R. Burnight, Arlene V. Drack, Bailey B. Banach, Dalyz Ochoa, Cathryn M. Cranston, Robert A. Madumba, Jade S. East, Robert F. Mullins, Edwin M. Stone, and Budd A. Tucker*

Department of Ophthalmology and Visual Sciences, Stephen A. Wynn Institute for Vision Research, Carver College of Medicine, University of Iowa, Iowa City, Iowa.

Juvenile neuronal ceroid lipofuscinosis (JNCL) is a childhood neurodegenerative disease with early-onset, severe central vision loss. Affected children develop seizures and CNS degeneration accompanied by severe motor and cognitive deficits. There is no cure for JNCL, and patients usually die during the second or third decade of life. In this study, independent lines of induced pluripotent stem cells (iPSCs) were generated from two patients with molecularly confirmed mutations in *CLN3*, the gene mutated in JNCL. Clinical-grade adeno-associated adenovirus serotype 2 (AAV2) carrying the full-length coding sequence of human *CLN3* was generated in a U.S. Food and Drug Administration-registered cGMP facility. AAV2-*CLN3* was efficacious in restoring full-length *CLN3* transcript and protein in patient-specific fibroblasts and iPSC-derived retinal neurons. When injected into the subretinal space of wild-type mice, purified AAV2-*CLN3* did not show any evidence of retinal toxicity. This study provides proof-of-principle for initiation of a clinical trial using AAV-mediated gene augmentation for the treatment of children with *CLN3*-associated retinal degeneration.

INTRODUCTION

The neuronal ceroid lipofuscinoses (NCLs) are a group of progressive neurodegenerative disorders that affect children and young adults.[1] To date, 14 different genetic subtypes of NCL, with ages of onset varying from infantile to adult, have been described.[2] The autosomal recessive juvenile form (JNCL), commonly known as Batten disease, is the most prevalent, presenting in roughly 1 in every 100,000 live births worldwide.[3] Although 59 different mutations in the gene *Ceroid Lipofuscinosis, Neuronal 3* (*CLN3*) have been reported to cause JNCL,[3] approximately 85% of patients harbor a 1-kb genomic deletion, which induces a frameshift and insertion of a premature stop codon, in at least one allele.[4] *CLN3* encodes a 438-amino acid hydrophobic protein of the same name, which is trafficked to, and expressed on, lysosomal membranes.[5,6] As mutations in *CLN3* lead to a buildup of autofluorescent lipofuscin-like deposits within the lysosomes of affected neuronal cells,[7] JNCL is often referred to as a "lysosomal storage" disorder.

CLN3-associated JNCL presents with rapidly progressive retinal degeneration that typically manifests between 4 and 7 years of age. Ophthalmoscopic findings include bull's eye maculopathy, optic nerve pallor, attenuated arterioles and peripheral retinal granularity. Within 2–5 years of diagnosis, patients usually experience profound vision loss that is due primarily to death of the light-sensing photoreceptor cells of the outer neural retina. In the ensuing decade, extensive death of CNS neurons leads to the onset of seizures, difficulty communicating, problems in walking, and ultimately death during the second or third decade of life. No U.S. Food and Drug Administration (FDA)-approved treatments currently exist for this fatal disease, but the fact that JNCL is a recessive disease, caused by variations in a gene expressed in the retina, raises the possibility of (1) lessening the

*Correspondence: Dr. Budd A. Tucker, Stephen A. Wynn Institute for Vision Research, Carver College of Medicine, University of Iowa, Department of Ophthalmology and Visual Sciences, 375 Newton Road, Iowa City, IA 52242. E-mail: budd-tucker@uiowa.edu

DOI: 10.1089/hum.2016.049

risk of recurrence of the disease in affected families through a combination of genetic counseling and preimplantation genetic testing, and (2) preventing neural cell death and disease progression via gene addition.

Adeno-associated virus (AAV)-based gene augmentation for the treatment of the retinal degenerative disorder *RPE65*-associated Leber congenital amaurosis has been highly successful.[8–10] A single subretinal injection of AAV2 (serotype 2) was shown to be well tolerated and sufficient to induce prolonged protein expression in humans.[11] Likewise, improvement in visual acuity, pupillary light reflex, visual fields, and ambulatory vision was detected as early as 2 weeks postinjection and was closely correlated with the area of the retina that received treatment.[11] No adverse immune responses or extraocular spread of AAV2-*RPE65* was detected.[11] These encouraging results, combined with the fact that AAV2 vectors have been shown to transduce both cone photoreceptor cells and inner retinal neurons,[12] suggests that this vector could be ideal for delivery of full-length *CLN3* as a means to mitigate disease progression and loss of vision in JNCL.

Advances in induced pluripotent stem cell (iPSC) technology have made it possible to generate patient-specific retinal photoreceptor cells *in vitro*.[13–19] These cells can be used both to evaluate the pathophysiology of newly identified genetic variants and to determine the efficacy of novel gene-based therapeutics.[20–22] In the case of rare diseases such as *CLN3*-associated JNCL, for which good animal models of retinal degeneration are lacking, the ability to generate patient-specific photoreceptor cells allows us to test whether AAV-based gene augmentation is capable of restoring wild-type transcript and protein without inducing overexpression toxicity in the patient for whom the treatment is intended. By combining this approach with *in vivo* toxicity studies in wild-type animals, one could significantly reduce the time between gene discovery and the first therapeutic trial in humans.

In this study, we generated independent iPSC lines from two patients with molecularly confirmed *CLN3*-associated JNCL: patient B775 (1.02-kb del/Leu101del3CTC) and patient B981 (1.02-kb del/c.1135_1138del). Clinical-grade AAV2 virus carrying full-length *CLN3* was generated in an FDA-registered facility using current good manufacturing practices (cGMP). Delivery of full-length *CLN3* via adeno-associated viral vector restored full-length *CLN3* transcript and protein to patient-specific fibroblasts and iPSC-derived retinal cells *in vitro*. On injection into wild-type mice, this purified virus demonstrated a complete lack of retinal toxicity. This study provides proof-of-principle for a single-eye gene augmentation trial in children with JNCL.

MATERIALS AND METHODS

Patients

This study was approved by the Institutional Review Board of the University of Iowa (project approval #199904167) and adhered to the tenets set forth in the Declaration of Helsinki. Patient reference numbers and corresponding molecularly confirmed *CLN3* mutations are as follows: patient B775 (1.02-kb del/Leu101del3CTC) and patient B967 (1.02-kb del/1.02-kb del).

Isolation of fibroblasts from patient dermal biopsies

Skin biopsies (3 mm) were obtained from either the non–sun-exposed upper arm or lower abdomen and minced in Iowa xeno-free (i.e., free of animal-derived products) biopsy medium, IxMedia. IxMedia consists of 395 ml of minimal essential medium (MEM)-α (Cat. No. 12571-063; Gibco/Thermo Fisher Scientific, Grand Island, NY), 50 ml of KnockOut serum replacement (Cat. No. 10828-028; Gibco/Thermo Fisher Scientific), 50 ml of heat-inactivated human serum (Cat. No. IPLA-SERAB-HI; Innovative Research, Novi, MI), 5 ml of GlutaMAX supplement (Cat. No. 35050-061; Gibco/Thermo Fisher Scientific), 1 ml of Primocin (Cat. No. ant-pm-2; InvivoGen, San Diego, CA), and recombinant human fibroblast growth factor-2 (rhFGF2) cGMP grade (10 ng/ml) (Cat. No. rhFGF; Waisman Biomanufacturing, Madison, WI). After mincing, tissue fragments were allowed to adhere to 6-well tissue culture-treated plates via air drying, and then cultured in IxMedia with 5% CO_2, 20% O_2 at 37°C. These cultures were fed every other day with 2 ml of fresh IxMedia per well. For the first two feedings, 1% extracellular matrix (ECM) mixture (human type 1 and type 3 collagen–vitronectin–fibronectin [Advanced BioMatrix, Carlsbad, CA]: collagen type 1 [Cat. No. 5007-20ML], collagen type 3 [Cat. No. 5021-MG], vitronectin [Cat. No. 5051-0.1MG], and fibronectin [Cat. No. 5050-1MG]) was added to the medium. Once cells reached confluence, they were passaged with xeno-free TrypLE Express (Cat. No. 12604-013; Life Technologies/Thermo Fisher Scientific, Grand Island, NY) and used to generate patient-specific iPSCs.

Patient-specific iPSC generation

Patient-specific dermal fibroblasts (250,000) were plated in 1 well of a 6-well culture dish with IxMedia. Twenty-four hours before transduction, medium was

switched to xeno-free, serum-free IxMedia. The next day, cells were transduced with nonintegrating Sendai viral vectors[16,17,19,23] driving expression of *OCT4*, *SOX2*, *KLF4*, and c-*MYC* at a multiplicity of infection (MOI) of 3 (CytoTune-iPS reprogramming kit, Cat. No. A16517; Invitrogen/Thermo Fisher Scientific, Waltham, MA) in viral transduction medium (serum-free IxMedia plus 50 μM Y-27632 ROCK inhibitor [Cat. No. 688000; EMD Millipore, Billerica, MA]). Transduction medium was removed 18 hr later and replaced daily with serum-free IxMedia. Five days after transduction, fibroblasts were passaged onto fresh xeno-free rLaminin-521 (human) (LN521)-coated 10-cm culture dishes (Cat. No. 354222; Corning Life Sciences, Tewksbury, MA) and fed with fresh serum-free IxMedia plus RevitaCell (Cat. No. A26445-01; Life Technologies/Thermo Fisher Scientific). On day 6, the medium was transitioned to xeno-free human Essential 6 (Cat. No. A1516401; Life Technologies/Thermo Fisher Scientific), using equal parts Essential 6 and serum-free IxMedia. From day 7 to day 21 cultures were fed daily with fresh Essential 6. On day 21, cultures were transitioned to human Essential 8 iPSC maintenance medium (Cat. No. A1517001; Life Technologies/Thermo Fisher Scientific) and fed daily. When iPSC colonies reached 1–2 mm in diameter they were manually isolated and passaged on fresh 12-well LN521-coated culture plates and clonally expanded in human Essential 8 medium. After expansion, cells were analyzed for pluripotency (i.e., expression of endogenous pluripotency factors) via rt-PCR and loss of transgene expression (i.e., lack of detectable expression of *OCT4*, *SOX2*, *KLF4*, or c-*MYC*), using a qPCR-based Scorecard assay.[24,25]

rt-PCR

Total RNA was isolated with an RNeasy mini kit (Cat. No. 74106; Qiagen, Germantown, MD) according to the manufacturer's instructions. One hundred nanograms of RNA template was amplified in one-step rt-PCRs, using the SuperScript III one-step RT-PCR system (Cat. No. 12574018; Life Technologies/Thermo Fisher Scientific) with primers hybridizing to human transcripts (listed in Table 1).

TaqMan human pluripotent stem cell Scorecard panel

Pluripotency of patient-derived iPSCs was assessed with the TaqMan human pluripotent stem cell Scorecard panel (Cat. Nos. A15870 and A15872; Life Technologies/Thermo Fisher Scientific).[24,25] Total RNA was isolated with an RNeasy mini kit (Qiagen) according to the manufacturer's instructions. One microgram of RNA was reverse transcribed with a SuperScript VILO cDNA synthesis kit (Cat. No. 11754050; Life Technologies/Thermo Fisher Scientific). cDNA was added to a human pluripotent stem cell (hPSC) Scorecard plate (Cat. No. A15870; Life Technologies/Thermo Fisher Scientific) and amplified with a QuantStudio 6 flex real-time PCR system with 384-well capability (Life Technologies/Thermo Fisher Scientific). Gene expression data were uploaded to the web-based hPSC Scorecard analysis software (Life Technologies/Thermo Fisher Scientific) for interpretation.

Table 1. *Primer sequences*

Human primer	*Sequence*
c-*MYC*-For	gctgcttagacgctggattt
c-*MYC*-Rev	agcagctcgaatttcttcca
KLF4-For	agaaggatctcggccaattt
KLF4-Rev	aagtcgcttcatgtgggaga
NANOG-For	ttcttccaccagtcccaaag
NANOG-Rev	ttgctccacattggaaggtt
OCT4-For	cgggttcaagtgattctcct
OCT4-Rev	agcttcctccacccacttct
SOX2-For	catcacccacagcaaatgac
SOX2-Rev	gcaaacttcctgcaaagctc
CLN3ex5-For	acatcctccccacactcgtcatc
CLN3ex11-Rev	acaatgtaccacagcagaccc
POLR2A-For	taacctgctgcggatgatctggaa
POLR2A-Rev	gatgttgaagagcagcgtggcatt

Two-dimensional differentiation of iPSC-derived photoreceptor precursor cells

Patient-derived iPSCs were cultured on ultralow-binding plates (Corning Life Sciences) in embryoid body formation medium (Dulbecco's modified Eagle's medium [DMEM] F-12 [Gibco/Thermo Fisher Scientific], 10% KnockOut serum replacement [Gibco/Thermo Fisher Scientific], 2% B27 supplement [Cat. No. 17504044; Gibco/Thermo Fisher Scientific], 1% N2 supplement [Cell Therapy Systems/Thermo Fisher Scientific], 1% L-glutamine [Cat. No. 25030081; Life Technologies/Thermo Fisher Scientific], 1× non-essential amino acids [NEAA; Life Technologies], 0.2% Primocin [InvivoGen], 1-ng/ml Dkk-1 [Cat. No. 5439-DK-010; R&D Systems, Minneapolis, MN], 1-ng/ml insulin-like growth factor [IGF]-I [Cat. No. 291-G1-200; R&D Systems], 1-ng/ml Noggin [Cat. No. 6057-NG-100; R&D Systems], and 0.5-ng/ml basic fibroblast growth factor [bFGF] [Cat. No. 233-FB-01M; R&D Systems]) for 4–5 days. Embryoid bodies (200–300 per well) were plated on 6-well plates (Corning Life Sciences) coated with 25-μg/ml collagen (Cat. No. 354265; BD Biosciences, San Jose, CA), 50-μg/ml laminin (Life Technologies/Thermo Fisher Scientific), and 100-μg/ml fibronectin (Sigma-Aldrich, St. Louis, MO) and cultured in dif-

ferentiation medium 1 (DMEM F-12 [Life Technologies], 2% B27 supplement [Gibco/Thermo Fisher Scientific], 1% N2 supplement [Life Technologies], 1% L-glutamine [Life Technologies/Thermo Fisher Scientific], 1×NEAA [Life Technologies], 0.2% Primocin [InvivoGen], 10-ng/ml Dkk-1 [R&D Systems], 10-ng/ml IGF-I [R&D Systems], 10-ng/ml Noggin [R&D Systems], and 5-ng/ml bFGF [R&D Systems]). Embryoid bodies were differentiated for 10 days followed by 6 days in differentiation medium 2 (differentiation medium 1 plus 10 μM *N*-[*N*-(3,5-difluorophenacetyl-L-alanyl)]-*S*-phenylglycine *t*-butyl ester [DAPT; EMD Millipore]) and for an additional 12 days of culture in differentiation medium 3 (differentiation medium 2 plus 2-ng/ml acidic fibroblast growth factor [aFGF] [Cat. No. 232-FA-025; R&D Systems]). Human photoreceptor precursors were cultured for an additional 60 days in differentiation medium 4 (DMEM F-12 [Life Technologies], 2% B27 supplement [Life Technologies], 1% N2 supplement [Life Technologies], 1% L-glutamine [Life Technologies/Thermo Fisher Scientific], 1×NEAA [Life Technologies], 0.2% Primocin [InvivoGen]).

Cloning of the transgene cassette plasmid carrying *CLN3*

AAV2, a member of the parvovirus family, is a nonpathogenic, helper-dependent single-stranded DNA virus. The expression cassette contains the minimal cytomegalovirus (CMV) promoter, the CMV immediate-early enhancer, and normal human full-length *CLN3* coding sequence. *CLN3* cDNA containing the coding sequence for human *CLN3* (NM_001042432; IDT-DNA Technologies, Coralville, IA) was cloned into the pFBAAVmcsBgHpA AAV2 plasmid backbone (provided by the University of Iowa Viral Vector Core Facility).[26] This plasmid backbone has the following characteristics: (1) it contains ampicillin and gentamicin resistance genes for selection and growth; (2) it contains a bacterial origin of replication (pUC); and (3) it contains inverted terminal repeats from AAV2. The final plasmid was sequence confirmed via bidirectional Sanger sequencing before packaging.

Treatment of patient fibroblasts and 2D iPSC-derived retinal precursor cells with AAV2-CMV-CLN3

Patient-specific iPSCs and imr90 control iPSCs were 2D differentiated[17,23] for 30 days. Retinal precursor cells were infected for 16 hr with AAV2-CMV-*CLN3* (viral titer, 1.63×10^{13}) at an MOI of 10,000. Sixteen hours postinfection, the cells were washed with fresh differentiation medium and fed every other day for 10 days. Ten days postinfection, cells were harvested for Western blot analysis. This same procedure was also performed on patient-specific fibroblasts.

Immunoblotting for CLN3

Western blots were performed as described previously.[16,17,20] Briefly, cells were treated with 0.25% trypsin–EDTA (Life Technologies), homogenized in lysis buffer (50 m*M* Tris-HCl [pH 7.6], 150 m*M* NaCl, 10 m*M* $CaCl_2$, 1% Triton X-100, 0.02% NaN_3 [Sigma-Aldrich]), and centrifuged. Supernatant protein concentrations were determined via bicinchoninic acid (BCA) assay according to the manufacturer's instructions (Pierce, Rockford, IL). Forty micrograms each was subjected to SDS–PAGE (4–20% Tris–glycine), transferred to polyvinylidene difluoride (PVDF), and probed with anti-CLN3 (diluted 1:1000) (Cat. No. ab75959; Abcam, Cambridge, UK). Alexa Fluor-conjugated secondary antibodies (Life Technologies) were used and blots were visualized fluorescently on a VersaDoc imaging system (Bio-Rad, Hercules, CA). Anti-GAPDH (glyceraldehyde-3-phosphate dehydrogenase, diluted 1:2000) (Cat. No. ab9483; Abcam) antibody was used as an internal loading control.

Clinical-grade, cGMP AAV production

AAV2-*CLN3* was manufactured under current Good Manufacturing Practices (cGMP) in the Steven W. Dezii Translational Vision Research Facility (DTVRF) within the Stephen A. Wynn Institute for Vision Research at the University of Iowa. This facility contains an independent high-efficiency particulate air (HEPA)-filtered equipment room, an ISO (International Organization for Standardization) class 7 (class 10,000) material storage and handling room, two ISO class 7 (class 10,000) gowning areas, two ISO class 6 (class 1000) processing rooms, and an unclassified service chase with dedicated access for equipment and facility maintenance. Each of the two processing rooms is equipped with custom BioSpherix Xvivo closed incubation systems, which are designed to exceed ISO class 5 (class 100) cleanliness requirements to ensure minimal biological contamination throughout standard operating procedures, while providing absolute optimal conditions for the long-term culturing of cells under defined atmospheric conditions.

AAV2-*CLN3* was manufactured using a characterized human HEK293T master cell line. To package the *CLN3* vector in AAV2 particles, HEK293T cells were transfected with a set of constructs encoding (1) normal human *CLN3* (pAAV2-CMV-*CLN3*, which contains the expression cassette flanked by AAV2 ITRs) and (2) AAV (pXX2-R2C2,

AAV2 packaging plasmid containing AAV2 *rep* and *cap* sequences) and helper virus-derived sequences (pHelper, containing *E2A* and *E4* genes from adenovirus serotype 2), which are required for packaging. Each of these plasmids was sequence confirmed via bidirectional sequencing before packaging in the DTVRF. HEK293T cells taken from a qualified Master Cell Bank (DTVRF HEK293T) were plated and expanded in T600 multilayer tissue culture flasks (production batch scale of 20 flasks). On reaching confluence, cells were simultaneously transfected with pAAV2-CMV-*CLN3*, pXX2-R2C2, and pHelper. To purify AAV2-*CLN3*, the following steps were performed: (1) HEK293T cultures were passaged and centrifuged to remove cell culture reagents and low molecular weight impurities; (2) HEK293T cells were lysed to release the intracellular vector, and nuclease digestion was performed to remove nucleic acid impurities; (3) cell debris was removed from the lysate via filtration, using 0.45- and 0.2-μm filters; (4) density gradient ultracentrifugation was performed to separate empty capsids (a major impurity) from the vector product; (5) affinity chromatography was performed using an ÄKTA Pure 25 chromatography system (GE Healthcare Life Sciences, Pittsburgh, PA) to purify vector; (6) viral particles were subsequently concentrated via buffer exchange; and (7) working concentrations of AAV2-*CLN3* were formulated in injection buffer (180 m*M* NaCl plus 10 m*M* Na_3PO_4 [trisodium phosphate] in water for injection at pH 7.2), filtered through a 0.2-μm filter, and vialed and labeled.

rt-PCR panel for virus contamination

Purified AAV2-*CLN3* was assessed by rt-PCR for viral contaminants of human, simian, bovine, and porcine origin. Briefly, total RNA was isolated with an RNeasy mini kit (Qiagen) according to the manufacturer's instructions. One microgram of RNA was reverse transcribed, using a SuperScript VILO cDNA synthesis kit (Cat. No. 11754050; Life Technologies/Thermo Fisher Scientific). Standard rt-PCR was performed with primers targeting the following viruses or contaminants: Human panel—AAV (adeno-associated virus), EBV (Epstein-Barr virus), CMV (cytomegalovirus), HBV (hepatitis B virus), HHV8 (human herpesvirus 8), HHV6 (human herpesvirus 6), HHV7 (human herpesvirus 7), HTLV1 (human T-lymphotropic virus 1), HTLV2 (human T-lymphotropic virus 2), parvovirus B19, HAV (hepatitis A virus), HCV (hepatitis C virus), and HIV (human immunodeficiency virus)[27–33]; simian panel—SFV (simian foamy virus), STLV (simian T-cell leukemia virus), SV40 (simian vacuolating virus 40), and SRV (simian retrovirus)[34–38]; 9CFR panel—BVDV (bovine viral diarrhea virus), MRV1 (mammalian reovirus 1), MRV2 (mammalian reovirus 2), MRV3 (mammalian reovirus 3), and rabies virus[39–41]; bovine panel—BMaAd (bovine mastadenovirus), BAtAd (bovine atadenovirus), BPV (bovine parvovirus), BTV (bluetongue virus), and BRSV (bovine respiratory syncytial virus)[42–44]; porcine panel—PAd (porcine adenovirus), PPV (porcine parvovirus), PHE-CoV (porcine hemagglutinating encephalomyelitis coronavirus), and TGEV (transmissible gastroenteritis virus).[45–48] gBlocks gene fragments (Integrated DNA Technologies, Coralville, IA) specific to each viral amplicon were designed to serve as positive controls.

Subretinal injection of AAV-CMV-CLN3

All animal procedures were approved by the University of Iowa's Animal Care and Use Committee. Ten C57BL/6J mice (Jackson Laboratory, Bar Harbor, ME) were anesthetized with ketamine–xylazine mixture and injected via the subretinal space as described previously[49] at 2 months of age. Right eyes received purified and concentrated clinical-grade cGMP AAV2-*CLN3* (10^9 vector genomes [VG]) in a volume of 1 μl and left eyes received the same dose of AAV2-*GFP* to serve as a contralateral control. Mice were sacrificed for histology 4 weeks after injection.

rt-PCR of vehicle- and AAV-CMV-*CLN3*-injected eyes

Ten C57BL/6J mice (Jackson Laboratory) were anesthetized with ketamine–xylazine mixture and injected via the subretinal space as described previously[49] at 2 months of age. Right eyes received purified and concentrated clinical-grade cGMP AAV2-*CLN3* (10^9 VG) in a volume of 1 μl and left eyes received sterile injection buffer (180 m*M* NaCl plus 10 m*M* Na_3PO_4 in water for injection at pH 7.2) to serve as a contralateral vehicle control. Mice were sacrificed for rt-PCR for human *CLN3* expression 3 weeks postinjection. Briefly, eyes were enucleated and posterior eyecups dissected from the anterior chamber. Whole retinas were then harvested for RNA isolation. Total RNA was isolated with an RNeasy mini kit (Cat. No. 74106; Qiagen) according to the manufacturer's instructions. One hundred nanograms of RNA template was used to generate cDNA, using a SuperScript VILO cDNA synthesis kit (Cat. No. 11754050; Thermo Fisher Scientific). Two hundred nanograms of cDNA was then amplified with primers hybridizing to human *CLN3* and *POLR2A* (listed in Table 1).

Histology of AAV2-*CLN3*-injected eyes

Mouse eyes were enucleated and fixed in 4% paraformaldehyde (PFA) for 2 hr and then embedded in paraffin. Paraffin-embedded eyes were sectioned, deparaffinized and counterstained with hematoxylin and eosin according to standard procedures.[16,17,20] Slides were masked as to whether they were from an AAV2-*CLN3*- or AAV2-*GFP*-injected eye. Slides were imaged with an EVOS XL Core microscope (Cat. No. AMEX1000; Life Technologies/Thermo Fisher Scientific) to assess retinas for AAV2-*CLN3*-mediated retinal toxicity. Retinal toxicity was assessed by measurement of the thickness of the outer nuclear layer, using ImageJ64 software (National Institutes of Health, Bethesda, MA). Ten random images (one from each of 10 different sections) were obtained by a person masked to the treatment groups in each of 10 AAV2-*CLN3*- or AAV2-*GFP*-injected eyes, for a total of 100 images per group. Outer nuclear layer thickness was measured in three different areas of each image and averaged for each treatment group. To assess uninjected wild-type retinas, outer nuclear layer thickness was measured in a section from the center of the globe from each of 10 eyes from 10 different C57BL/6J mice. A paired, two-tailed Student *t* test was performed to determine significance, using Prism 6 (Graphpad Software, La Jolla, CA). $p < 0.05$ was considered statistically significant.

RESULTS

Generation of patient-specific *CLN3*-associated JNCL iPSCs

To test the efficacy of virus-mediated correction of *CLN3* disease *in vitro*, we first generated patient-derived iPSCs and iPSC-derived neuronal retinal precursor cells. Skin biopsies were acquired from

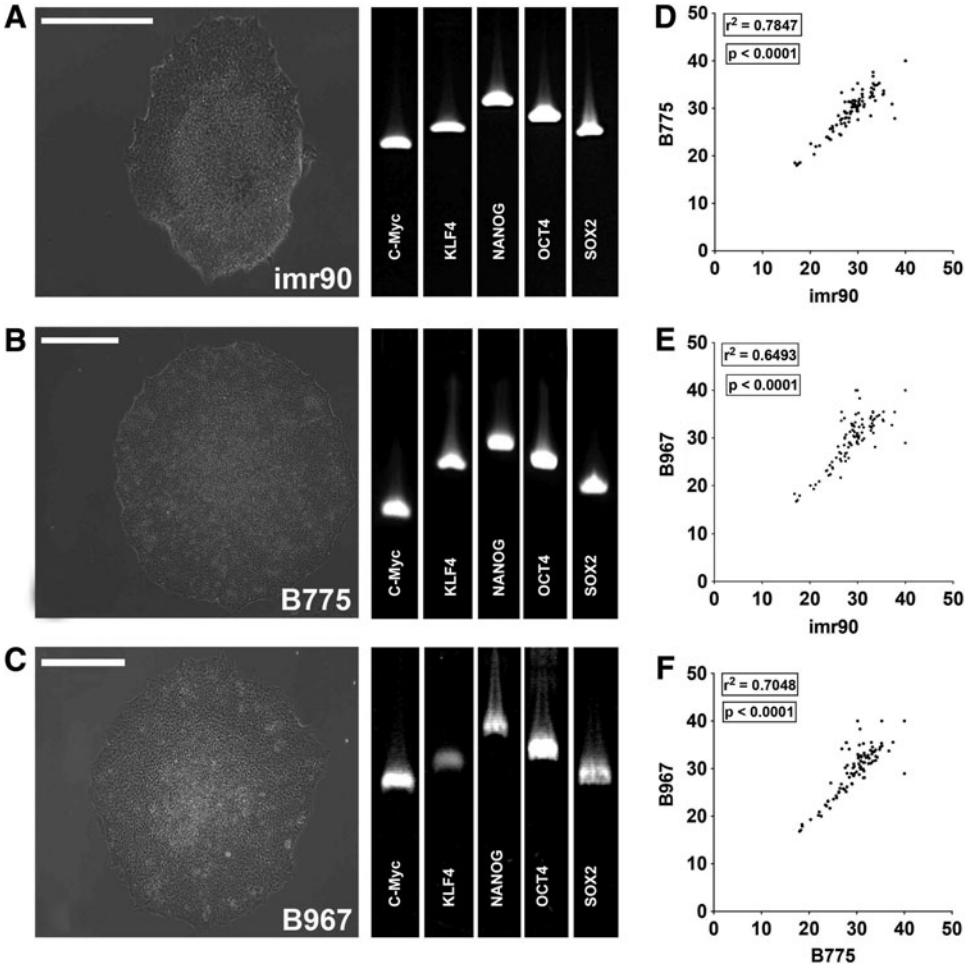

Figure 1. Generation and characterization of induced pluripotent stem cells (iPSCs) from patients with *CLN3*-associated juvenile neuronal ceroid lipofuscinosis (JNCL). **(A–C)** Representative light micrographs of iPSC colonies and rt-PCR for standard pluripotency markers from control iPSC line imr90 **(A)** and two *CLN3* patient lines, B775 **(B)** and B967 **(C)**. **(D** and **E)** Pair-wise comparison of all C_t values for genes tested in each line. Scatter plots are shown comparing each line with one another, with corresponding correlation coefficients and *p* values: imr90 versus B775 (**D**; $r^2 = 0.7847$; $p < 0.0001$), imr90 versus B967 (**E**; $r^2 = 0.6493$; $p < 0.0001$), and B775 versus B967 (**F**; $r^2 = 0.7048$; $p < 0.0001$). Scale bars: 400 μm.

two patients with molecularly confirmed mutations in *CLN3*: patient B775 (compound heterozygote; 1.02-kb del/Leu101del3CTC) and patient B967 (homozygote; 1.02-kb del/1.02-kb del). The imr90 (WiCell Research Institute, Madison, WI) human iPSC line was used as a nondisease control. Fibroblasts were isolated, cultured, and reprogrammed as induced pluripotent stem cells (iPSCs) via viral transduction of the transcription factors *OCT4*, *SOX2*, *KLF4*, and c-*MYC* as previously described.[16,17,19,23] Approximately 3 weeks after transduction, densely packed colonies of cells with a high nucleus-to-cytoplasm ratio (Fig. 1A–C) were isolated and clonally expanded. After 10 passages expression of the pluripotency transcripts c-*MYC*, *KLF4*, *NANOG*, *OCT4*, and *SOX2* was confirmed via rt-PCR (Fig. 1A–C). Pluripotency was further assessed with the newly available TaqMan human pluripotent stem cell Scorecard panel.[24,25] This assay uses real-time PCR to compare transcript expression levels required for self-renewal, ectoderm, mesoderm, or endoderm formation in lines of interest to an undifferentiated iPSC reference gene set. Pair-wise comparison of all C_t values for genes tested showed that imr90, B775, and B967 were pluripotent and transcriptionally similar to one another as demonstrated by scatter plots and correlation coefficients (Fig. 1D–F; imr90 vs. B775 = 0.7847, $p < 0.0001$; imr90 vs. B967 = 0.6493, $p < 0.0001$; B775 vs. B967 = 0.7048, $p < 0.0001$). Taken together, these data show that we had successfully generated two independent, iPSC lines from patients with *CLN3* mutations and a human control iPSC line.

AAV2-*CLN3* restores full-length CLN3 protein in patient-specific iPSC-derived retinal cells

After successfully generating patient-specific iPSCs, we differentiated these lines to develop iPSC-derived retinal cells to test the ability of adeno-associated viral particles carrying wild-type, full-length *CLN3* (Table 1) to restore expression of CLN3 protein. For these experiments, we used a two-dimensional differentiation protocol that we have previously demonstrated for the development of patient-specific retinal cells (Fig. 2C, inset).[16,17] The AAV we chose for these studies was the serotype 2 AAV vector designed with a CMV promoter driving *CLN3* gene expression (Fig. 2A). This AAV vector is the same serotype that has been successfully used in clinical human gene augmentation trials to treat *RPE65*-associated Leber congenital amaurosis.[8,11,50] Initially, to test the ability of this vector to drive *CLN3* transcript, we transduced *CLN3* patient fibroblasts and performed rt-PCR using primers specific to human *CLN3*. Little (B775) or no (B967) *CLN3* transcript was detected in fibroblasts derived from either patient with JNCL before transduction (Fig. 2B). AAV2-*CLN3* was able to drive and restore robust expression of *CLN3* transcript in the cells of both patients (Fig. 2B). To test the efficacy of AAV2-*CLN3* in restoring full-length CLN3 protein in patient-specific retinal neurons, we differentiated patient iPSCs for 30 days, the time point at which neuronal rosettes are clearly visible in differentiating cultures (Fig. 2C, inset). To assess CLN3 protein levels we produced an immunoblot, using a human anti-CLN3 antibody. CLN3 was robustly expressed in whole retinal protein lysate isolated from a human donor eye, as expected (Fig. 2C, H. Ret).

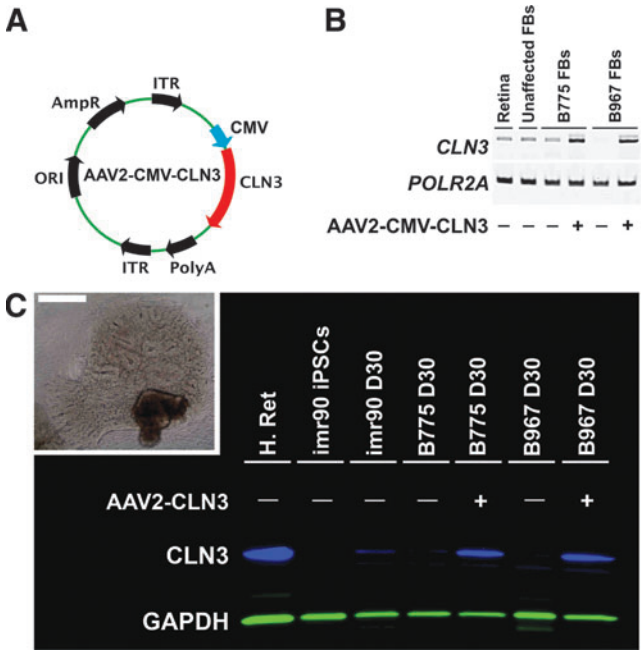

Figure 2. Transduction of patient-specific fibroblasts and two-dimensional (2D) iPSC-derived retinal neurons restores expression of CLN3. **(A)** Vector diagram of AAV2-*CLN3* used to transduce patient fibroblasts and iPSC-derived retinal neurons. **(B)** rt-PCR panel comparing transcripts from human retina (Retina), unaffected human foreskin-derived fibroblasts (Unaffected FBs), and skin fibroblasts from two patients with *CLN3*-associated disease, B775 (B775 FBs) and B967 (B967 FBs). Results are shown for *CLN3* (primers flanking exons 5–12) and the housekeeping gene, *POLR2A*. Transduction of patient fibroblasts with AAV2-CMV-*CLN3* restores *CLN3* transcript compared with untransduced fibroblasts. **(C)** Western blot comparing unaffected human donor retinal lysate (H. Ret), undifferentiated imr90 iPSCs, imr90 cells differentiated for 30 days (imr90 D30), and B775 and B967 patient cells differentiated for 30 days with and without addition of AAV2-*CLN3*. Transduction of iPSC-derived retinal neurons with AAV2-*CLN3* rescued full-length CLN3 protein (*blue*) in both patient lines. Anti-GAPDH (*green*) was used as an internal loading control. *Inset:* A typical neural retina-like structure with retinal pigment epithelium (RPE) pigmentation and numerous neural rosettes. Scale bar: 400 μm. ORI, origin of replication; AmpR, ampicillin resistance cassette; ITR, inverted terminal repeats; CMV, cytomegalovirus promoter; CLN3, full-length CLN3 cDNA; PolyA, polyadenylation signal.

Neurons from an unaffected control patient, imr90, at 30 days postdifferentiation expressed CLN3, whereas undifferentiated iPSCs did not (Fig. 2C, imr90 iPSCs vs. imr90 D30). AAV2-*CLN3* restored full-length CLN3 protein to retinal neurons derived from both *CLN3* patients, B775 and B967, compared with uninfected differentiated neurons (Fig. 2C). These data demonstrate that we successfully cloned and packaged an AAV vector driving *CLN3* and that this vector is efficacious in restoring full-length *CLN3* transcript and protein to patient-specific neural progenitor cells.

Production of clinical-grade cGMP AAV2-*CLN3*

After demonstrating that AAV2-*CLN3* successfully restores full-length transcript and protein to patient-derived cells, we next sought to produce this vector in a clinical-grade manner suitable for use in clinical trials in children with *CLN3* JNCL. To achieve this, we produced AAV2-*CLN3* under cGMP conditions in an onsite, FDA-registered cGMP facility. This facility exceeds ISO class 5 (class 100) cleanliness requirements to ensure minimal biological contamination throughout standard operating procedures, while providing optimal conditions for the long-term culturing of cells under defined atmospheric conditions.

AAV2-*CLN3* was manufactured with a characterized human HEK293T master cell line. HEK293T cells were transfected with a transgene cassette plasmid AAV2-CMV-*CLN3*, an AAV2 packaging plasmid containing AAV2 *rep* and *cap* sequences, and a plasmid carrying helper virus-derived sequences (pHelper, containing *E2A* and *E4* genes from adenovirus serotype 2). To purify AAV2-*CLN3*, HEK293T cultures were passaged and centrifuged to remove cell culture reagents and

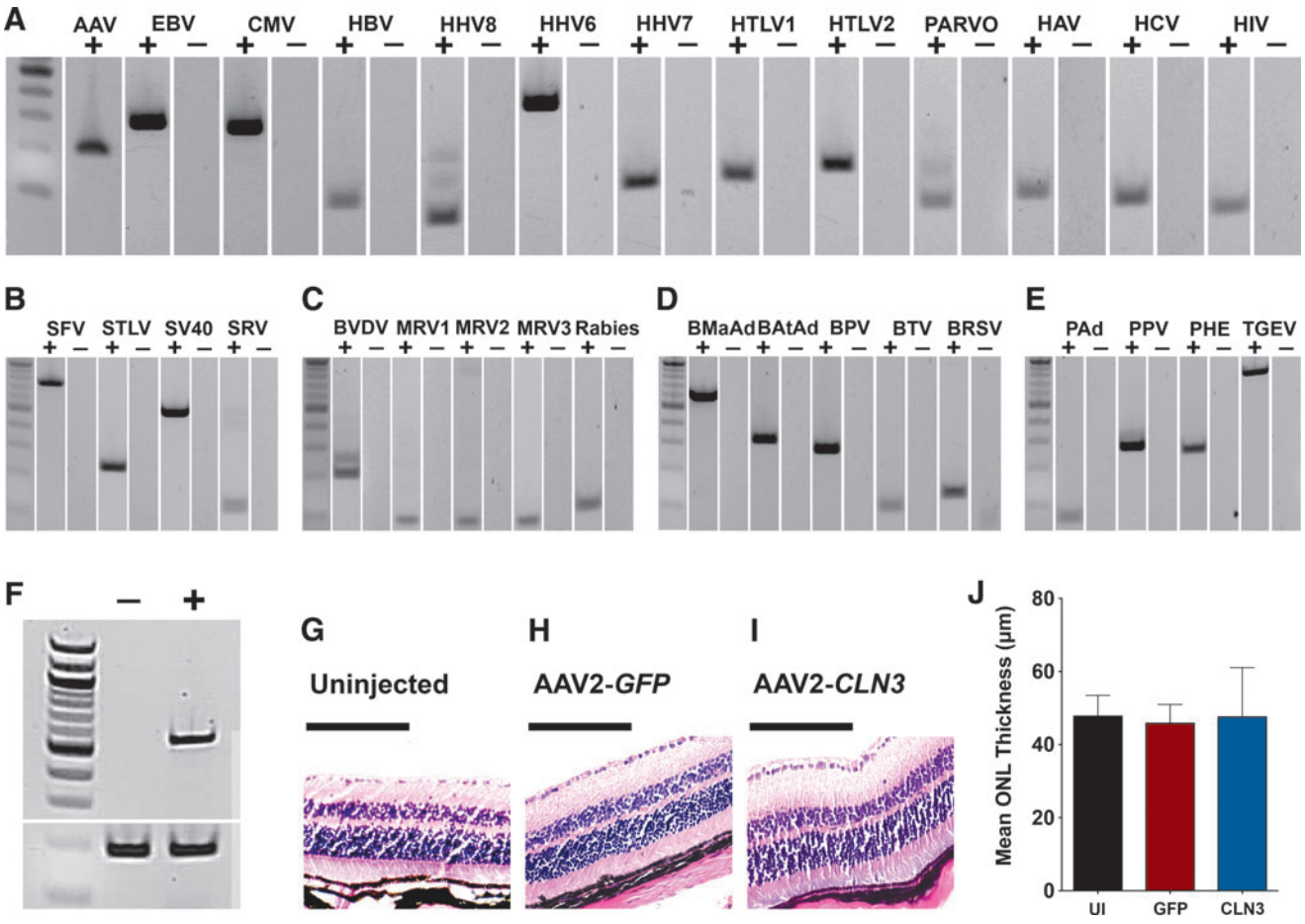

Figure 3. Purified AAV2-*CLN3* displays a lack of retinal toxicity in wild-type mice. **(A–E)** rt-PCR for virus panels specific for human **(A)**, simian **(B)**, required code of federal regulations **(C)**, bovine **(D)**, and porcine **(E)** viruses and contaminants in purified AAV2-*CLN3*. **(F)** rt-PCR for human *CLN3* (*top band*) and *POLR2A* (*bottom band*) in mouse eyes injected with sterile buffer only (–) or AAV2-*CLN3* (+) at 3 weeks postinjection. **(G–I)** Representative hematoxylin- and eosin-stained paraffin sections from uninjected **(G)**, AAV2-*GFP*-injected **(H)**, and AAV2-*CLN3*-injected **(I)** eyes. **(J)** Histogram comparing the mean thickness of the outer nuclear layer (ONL) between uninjected ($n=10$ eyes), AAV2-*GFP*-injected ($n=10$ eyes), and AAV2-*CLN3*-injected ($n=10$ eyes) mice (AAV2-*GFP* vs. AAV2-*CLN3*, $p=0.72$). Scale bars: 100 μm.

low molecular weight impurities and lysed and digested to release the intracellular vector and remove nucleic acid impurities. Cellular debris was removed from the lysate via filtration followed by density gradient ultracentrifugation to separate empty capsids (a major impurity) from the vector product. Finally, affinity chromatography was performed to purify the vector and AAV2-*CLN3* was subsequently concentrated via buffer exchange. To demonstrate the purity of AAV2-*CLN3*, we performed a series of rt-PCRs to assess the presence of viruses and vector contaminants. As demonstrated in Fig. 3, AAV2-*CLN3* was completely devoid of viral DNA of human (Fig. 3A), simian (Fig. 3B), bovine (Fig. 3D), and porcine origin (Fig. 3E). AAV2-*CLN3* also lacked expression of all viruses specified by the code of federal regulations (Fig. 3C).

To demonstrate that subretinal injection of AAV2-*CLN3* transduced neural retina, we injected wild-type C57BL/6J mice with either sterile injection buffer ($n=10$) or 10^9 VG of AAV2-*CLN3* ($n=10$). At 3 weeks postinjection rt-PCR, using primers specific for human *CLN3*, showed robust expression of *CLN3* transcript in AAV2-*CLN3*-injected retinas as compared with vehicle-injected controls (Fig. 3F). With a highly pure and concentrated AAV2-*CLN3* vector in hand, we next asked whether delivery of *CLN3*, at a viral titer exceeding that which would likely be tested in humans, would be toxic when injected into wild-type murine retinas. We injected wild-type C57BL/6J mice with either 10^9 VG of AAV2-*GFP* ($n=10$ right eyes) or 10^9 VG of AAV2-*CLN3* ($n=10$ left eyes) and assessed retinal histology 2 months postinjection. Uninjected wild-type eyes were used as an additional control to ensure there was no green fluorescent protein (GFP)-induced retinal toxicity (Fig. 3G). Vector-induced toxicity was assessed by measuring and comparing the mean thickness of the outer nuclear layer between treatment groups. Mean outer nuclear layer thickness did not differ between AAV2-*GFP*- and AAV2-*CLN3*-injected eyes (Fig. 3J; $p=0.72$). Likewise, hematoxylin- and eosin-stained sections were morphologically identical between uninjected (Fig. 3G), AAV2-*GFP*-injected (Fig. 3H), and AAV2-*CLN3*-injected eyes (Fig. 3I). Together, these data demonstrate the production of a highly pure, potent, and safe cGMP-compliant clinical-grade AAV2-*CLN3* vector.

DISCUSSION

In this study we describe the generation of clinical-grade, cGMP-compliant patient-specific iPSCs from two individuals with *CLN3*-associated retinal degeneration. We demonstrate the usefulness of these cells for testing the efficacy of a clinical-grade AAV-mediated gene augmentation strategy. Furthermore, we show that AAV2-*CLN3* is nontoxic to mouse retinas when delivered *in vivo*. We propose that these data provide proof-of-concept for the design and initiation of a clinical trial in children with *CLN3* JNCL disease.

Nonintegrating AAV2 has been successfully used as a clinical gene transfer vehicle to treat human retinal degenerative disease.[10,11,50–53] It has been established that AAV2 is safe, well tolerated, and restricted to the eye after subretinal delivery.[11,50,51,53–55] For example, AAV2 carrying the *RPE65* gene has been reproducibly demonstrated to be safe and beneficial for the treatment of *RPE65*-associated Leber congenital amaurosis.[10,11,51–54] The safety and efficacy profile of AAV2, coupled with the fact that this vector is capable of carrying full-length *CLN3*, and has been shown to be capable of transducing both cone photoreceptor and inner retinal neurons,[12] makes it a logical choice for the treatment of JNCL.

The retina is a highly specialized extension of the brain derived from the neural ectoderm.[56] Like the cerebral cortex, it is an organized, laminated structure, consisting of a diverse mixture of neurons and glia. Similarities between the neural retina and the cerebral cortex suggest that success of a gene augmentation-based approach in the eye could serve as proof-of-principle for a similar treatment in the brain. *In vivo* animal studies assessing both the efficacy and safety of AAV-mediated gene delivery to the brain have been demonstrated for two forms of NCL: infantile NCL (caused by mutations in the gene *PPT1*) and late infantile NCL (caused by mutations in the gene *TPP1*). AAV delivery of *TPP1* to the brain has been demonstrated in mice,[57–59] rats,[60] nonhuman primates,[60] and canines.[61] Likewise, one group has demonstrated the efficacy of AAV-mediated delivery of *PPT1* in murine eyes[62] before showing that CNS delivery ameliorated functional deficits in the same *Ppt1*$^{-/-}$ mouse.[63] Importantly, AAV2-mediated treatment of 10 children with *TPP1*-associated late infantile NCL, administered throughout the CNS, slowed disease progression.[64] These studies have laid the groundwork for similar treatment of children with *CLN3* disease.

If AAV-mediated therapy is found to be safe and effective in the eye, then delivery of AAV2-*CLN3* to the brain would be the next logical step. Although observing efficacy in the eyes of these children would be a great achievement, and would significantly reduce the suffering from this disease, blindness is only one of the problems faced by

patients with JNCLs. Development of a treatment that could be used to slow or prevent the cognitive decline, onset of seizures, and loss of motor function associated with JNCL is the ultimate goal. Unlike the genes *TPP1* and *PPT1*, both of which transcribe soluble enzymes,[58,63,65–67] *CLN3* encodes an intracellular protein that is localized to the membrane of lysosomes. Unfortunately, this means that compared with *TPP1*- or *PPT1*-associated NCL, which can be effectively treated by transducing a relatively small number of cells and relying on the secreted gene product to induce a widespread rescue effect, for *CLN3* gene augmentation to be effective it is likely that extensive CNS transduction will be necessary. Although AAV2-based transduction of cone photoreceptor cells and inner retinal neurons may be sufficient to prevent vision loss, it is likely that a serotype such as AAV9, which has been demonstrated to be significantly better at transducing CNS neurons,[68,69] will be required. Even then, to treat the entire CNS, one would need to deliver a large quantity of viral vector by some means, perhaps by repeated intrathecal injection. Whether a patient could tolerate such treatments, and whether they could ameliorate the condition sufficiently to make it worthwhile, are completely unknown at the present time.

An alternative approach would be to identify systemically active compounds, perhaps even orally deliverable, that would act to slow or halt disease progression. As JNCL has been demonstrated to have an autoimmune component, several groups have attempted to use various immunosuppressive agents for this purpose.[70] For instance, Seehafer and colleagues demonstrated that the immunomodulatory compound mycophenolate mofetil (trade name CellCept), when given to *Cln3*$^{-/-}$ mice, decreased immunoglobulin G deposition, promoted cell survival, and improved motor function.[71] A phase 2 clinical trial designed to evaluate the usefulness of this compound in children with *CLN3* JNCL is currently underway (clinical trial NCT01399047).[70] As promising as these findings are, immunosuppressive agents are less than ideal. They decrease the patient's ability to respond to infections,[72] increase the chance of developing cancer,[73] and can cause injury to vital organs.[74] Although animal models of disease are valuable for testing therapeutic efficacy, large-scale screening for compounds that may be capable of altering disease progression will require *in vitro* models such as patient-specific iPSCs that recapitulate key disease phenotypes such as autofluorescent lysosomal storage granules.

Many patients with JNCL have retinal disease that has progressed beyond the point at which gene replacement therapy would be beneficial. For these patients, transplantation of iPSC-derived photoreceptor precursors may eventually be able to restore some of their vision. For autologous cell replacement therapy, one would first need to correct the *CLN3* mutations to prevent the newly transplanted cells from suffering the same fate as the original ones. This is particularly important for JNCL because of its early onset and aggressive photoreceptor death. Fortunately, advances in CRISPR/Cas9-mediated genome editing now allow the highly specific correction of disease-causing alleles in patient-specific stem cells. As *CLN3*-associated JNCL is inherited in an autosomal recessive fashion, correction of either of a patient's disease-causing alleles should be sufficient. It is advantageous that the most common mutation in *CLN3*, a 1-kb genomic deletion, occurs in approximately 85% of patients.[4] For example, the two patients investigated in this study each harbor this mutation: one heterozygously and the other homozygously. Designing a strategy to correct this variant would allow for the production of healthy, immunologically matched photoreceptor precursor cells for use in cell replacement therapy.

In conclusion, we have demonstrated the development of a clinical-grade AAV2 vector that is capable of restoring full-length *CLN3* transcript and protein to retinal cells derived from two patients with *CLN3*-associated JNCL. Furthermore, AAV2-*CLN3* is safe in the eyes of wild-type mice, displaying a complete lack of vector-induced overexpression toxicity. This study provides preclinical data for the use of AAV2-*CLN3* to treat retinal degenerative blindness caused by mutations in the gene *CLN3*.

ACKNOWLEDGMENTS

The authors thank the patients for their participation in this research study. This work was supported by grants from the Stephen A. Wynn Foundation, the Elmer and Sylvia Sramek Charitable Foundation, the National Institutes of Health (1-DP2-OD007483-01, EY-024605, and EY-024588), Research to Prevent Blindness, and the Foundation Fighting Blindness.

AUTHOR DISCLOSURE

No competing financial interests exist.

REFERENCES

1. Mole SE, Cotman SL. Genetics of the neuronal ceroid lipofuscinoses (Batten disease). Biochim Biophys Acta 2015;1852:2237–2241.
2. Kmoch S, Stránecký V, Emes RD, et al. Bioinformatic perspectives in the neuronal ceroid lipofuscinoses. Biochim Biophys Acta 2013;1832: 1831–1841.
3. Drack AV, Miller JN, Pearce DA. A Novel c.1135_1138delCTGT mutation in *CLN3* leads to juvenile neuronal ceroid lipofuscinosis. J Child Neurol 2013;28:1112–1116.
4. de los Reyes E, Dyken PR, Phillips P, et al. Profound infantile neuroretinal dysfunction in a heterozygote for the *CLN3* genetic defect. J Child Neurol 2004;19:42–46.
5. Margraf LR, Boriack RL, Routheut AA, et al. Tissue expression and subcellular localization of CLN3, the Batten disease protein. Mol Genet Metab 1999;66:283–289.
6. Mao Q, Xia H, Davidson BL. Intracellular trafficking of CLN3, the protein underlying the childhood neurodegenerative disease, Batten disease. FEBS Lett 2003;555:351–357.
7. Gardiner M, Sandford A, Deadman M, et al. Batten disease (Spielmeyer-Vogt disease, juvenile onset neuronal ceroid-lipofuscinosis) gene (*CLN3*) maps to human chromosome 16. Genomics 1990; 8:387–390.
8. Maguire AM, High KA, Auricchio A, et al. Age-dependent effects of *RPE65* gene therapy for Leber's congenital amaurosis: a phase 1 dose-escalation trial. Lancet 2009;374:1597–1605.
9. Stein L, Roy K, Lei L, et al. Clinical gene therapy for the treatment of RPE65-associated Leber congenital amaurosis. Expert Opin Biol Ther 2011; 11:429–439.
10. Jacobson SG, Cideciyan AV, Ratnakaram R, et al. Gene therapy for Leber congenital amaurosis caused by *RPE65* mutations: safety and efficacy in 15 children and adults followed up to 3 years. Arch Ophthalmol 2012;130:9–24.
11. Maguire AM, Simonelli F, Pierce EA, et al. Safety and efficacy of gene transfer for Leber's congenital amaurosis. N Engl J Med 2008;358:2240–2248.
12. Watanabe S, Sanuki R, Ueno S, et al. Tropisms of AAV for subretinal delivery to the neonatal mouse retina and its application for *in vivo* rescue of developmental photoreceptor disorders. PLoS One 2013;8:e54146.
13. Jin Z-B, Okamoto S, Osakada F, et al. Modeling retinal degeneration using patient-specific induced pluripotent stem cells. PLoS One 2011;6: e17084.
14. Singh R, Shen W, Kuai D, et al. iPS cell modeling of Best disease: insights into the pathophysiology of an inherited macular degeneration. Hum Mol Genet 2013;22:593–607.
15. Phillips MJ, Perez ET, Martin JM, et al. Modeling human retinal development with patient-specific induced pluripotent stem cells reveals multiple roles for visual system homeobox 2. Stem Cells 2014;32:1480–1492.
16. Tucker BA, Scheetz TE, Mullins RF, et al. Exome sequencing and analysis of induced pluripotent stem cells identify the cilia-related gene male germ cell-associated kinase (MAK) as a cause of retinitis pigmentosa. Proc Natl Acad Sci USA 2011;108:E569–E576.
17. Tucker BA, Mullins RF, Streb LM, et al. Patient-specific iPSC-derived photoreceptor precursor cells as a means to investigate retinitis pigmentosa. Elife 2013;2:e00824.
18. Tucker BA, Cranston C, Anfinson KR, et al. Using patient specific iPSCs to interrogate the pathogenicity of a novel RPE65 cryptic splice site mutation and confirm eligibility for enrollment into a clinical gene augmentation trial. Transl Res 2015;166:740–749.e1.
19. Small KW, DeLuca AP, Whitmore SS, et al. North Carolina macular dystrophy is caused by dysregulation of the retinal transcription factor PRDM13. Ophthalmology 2015;123:9–18.
20. Burnight ER, Wiley LA, Drack AV, et al. *CEP290* gene transfer rescues Leber congenital amaurosis cellular phenotype. Gene Ther 2014;21:662–672.
21. Cereso N, Pequignot MO, Robert L, et al. Proof of concept for AAV2/5-mediated gene therapy in iPSC-derived retinal pigment epithelium of a choroideremia patient. Mol Ther Methods Clin Dev 2014;1:14011.
22. Vasireddy V, Mills JA, Gaddameedi R, et al. AAV-mediated gene therapy for choroideremia: preclinical studies in personalized models. PLoS One 2013;8:e61396.
23. Tucker BA, Anfinson KR, Mullins RF, et al. Use of a synthetic xeno-free culture substrate for induced pluripotent stem cell induction and retinal differentiation. Stem Cells Transl Med 2013;2: 16–24.
24. Tsankov AM, Akopian V, Pop R, et al. A qPCR ScoreCard quantifies the differentiation potential of human pluripotent stem cells. Nat Biotechnol 2015;33:1182–1192.
25. Fergus J, Quintanilla R, Lakshmipathy U. Characterizing pluripotent stem cells using the TaqMan hPSC Scorecard panel. Methods Mol Biol 2016;1307:25–37.
26. Urabe M, Ding C, Kotin RM. Insect cells as a factory to produce adeno-associated virus type 2 vectors. Hum Gene Ther 2002;13:1935–1943.
27. Engelmann I, Petzold DR, Kosinska A, et al. Rapid quantitative PCR assays for the simultaneous detection of herpes simplex virus, varicella zoster virus, cytomegalovirus, Epstein-Barr virus, and human herpesvirus 6 DNA in blood and other clinical specimens. J Med Virol 2008; 80:467–477.
28. Kodani M, Mixson-Hayden T, Drobeniuc J, et al. Rapid and sensitive approach to simultaneous detection of genomes of hepatitis A, B, C, D and E viruses. J Clin Virol 2014;61:260–264.
29. Watzinger F, Suda M, Preuner S, et al. Real-time quantitative PCR assays for detection and monitoring of pathogenic human viruses in immunosuppressed pediatric patients. J Clin Microbiol 2004;42:5189–5198.
30. Lawrence DC, Stover CC, Noznitsky J, et al. Structure of the intact stem and bulge of HIV-1 Psi-RNA stem-loop SL1. J Mol Biol 2003;326:529–542.
31. Styer LM, Miller TT, Parker MM. Validation and clinical use of a sensitive HIV-2 viral load assay that uses a whole virus internal control. J Clin Virol 2013;58(Suppl 1):e127–e133.
32. Pripuzova N, Wang R, Tsai S, et al. Development of real-time PCR array for simultaneous detection of eight human blood-borne viral pathogens. PLoS One 2012;7:e43246.
33. Costa C, Terlizzi ME, Solidoro P, et al. Detection of parvovirus B19 in the lower respiratory tract. J Clin Virol 2009;46:150–153.
34. Switzer WM, Bhullar V, Shanmugam V, et al. Frequent simian foamy virus infection in persons occupationally exposed to nonhuman primates. J Virol 2004;78:2780–2789.
35. Schweizer M, Neumann-Haefelin D. Phylogenetic analysis of primate foamy viruses by comparison of *pol* sequences. Virology 1995;207:577–582.
36. White JA, Todd PA, Rosenthal AN, et al. Development of a generic real-time PCR assay for simultaneous detection of proviral DNA of simian betaretrovirus serotypes 1, 2, 3, 4 and 5 and secondary uniplex assays for specific serotype identification. J Virol Methods 2009;162:148–154.
37. Van Dooren S, Shanmugam V, Bhullar V, et al. Identification in gelada baboons (*Theropithecus gelada*) of a distinct simian T-cell lymphotropic virus type 3 with a broad range of Western blot reactivity. J Gen Virol 2004;85:507–519.
38. Fagrouch Z, Karremans K, Deuzing I, et al. Molecular analysis of a novel simian virus 40 (SV40) type in rhesus macaques and evidence for double infections with the classical SV40 type. J Clin Microbiol 2011;49:1280–1286.
39. Wernike K, Hoffmann B, Beer M. Simultaneous detection of five notifiable viral diseases of cattle by single-tube multiplex real-time RT-PCR. J Virol Methods 2015;217:28–35.
40. Gallagher EM, Margolin AB. Development of an integrated cell culture—real-time RT-PCR assay for detection of reovirus in biosolids. J Virol Methods 2007;139:195–202.
41. Wacharapluesadee S, Tepsumethanon V, Supavonwong P, et al. Detection of rabies viral RNA by TaqMan real-time RT-PCR using non-neural specimens from dogs infected with rabies virus. J Virol Methods 2012;184:109–112.

42. Sibley SD, Goldberg TL, Pedersen JA. Detection of known and novel adenoviruses in cattle wastes via broad-spectrum primers. Appl Environ Microbiol 2011;77:5001–5008.

43. Bae JE, Kim IS. Multiplex PCR for rapid detection of minute virus of mice, bovine parvovirus, and bovine herpesvirus during the manufacture of cell culture-derived biopharmaceuticals. Biotechnol Bioproc Eng 2011;15:1031–1037.

44. Thonur L, Maley M, Gilray J, et al. One-step multiplex real time RT-PCR for the detection of bovine respiratory syncytial virus, bovine herpesvirus 1 and bovine parainfluenza virus 3. BMC Vet Res 2012;8:37.

45. Hundesa A, Maluquer de Motes C, Albinana-Gimenez N, et al. Development of a qPCR assay for the quantification of porcine adenoviruses as an MST tool for swine fecal contamination in the environment. J Virol Methods 2009;158:130–135.

46. Zeng Z, Liu Z, Wang W, et al. Establishment and application of a multiplex PCR for rapid and simultaneous detection of six viruses in swine. J Virol Methods 2014;208:102–106.

47. Zhao J, Shi B-J, Huang X-G, et al. A multiplex RT-PCR assay for rapid and differential diagnosis of four porcine diarrhea associated viruses in field samples from pig farms in East China from 2010 to 2012. J Virol Methods 2013;194:107–112.

48. Quiroga MA, Cappuccio J, Piñeyro P, et al. Hemagglutinating encephalomyelitis coronavirus infection in pigs, Argentina. Emerging Infect Dis 2008;14:484–486.

49. Seo S, Mullins RF, Dumitrescu AV, et al. Subretinal gene therapy of mice with bardet-biedl syndrome type 1. Invest Ophthalmol Vis Sci 2013;54:6118–6132.

50. Jacobson SG, Acland GM, Aguirre GD, et al. Safety of recombinant adeno-associated virus type 2-RPE65 vector delivered by ocular subretinal injection. Mol Ther 2006;13:1074–1084.

51. Simonelli F, Maguire AM, Testa F, et al. Gene therapy for Leber's congenital amaurosis is safe and effective through 1.5 years after vector administration. Mol Ther 2010;18:643–650.

52. Bennett J, Ashtari M, Wellman J, et al. AAV2 gene therapy readministration in three adults with congenital blindness. Sci Transl Med 2012;4:120ra15.

53. Testa F, Maguire AM, Rossi S, et al. Three-year follow-up after unilateral subretinal delivery of adeno-associated virus in patients with Leber congenital amaurosis type 2. Ophthalmology 2013;120:1283–1291.

54. Jacobson SG, Boye SL, Aleman TS, et al. Safety in nonhuman primates of ocular AAV2-RPE65, a candidate treatment for blindness in Leber congenital amaurosis. Hum Gene Ther 2009;17:845–858.

55. Barker SE, Broderick CA, Robbie SJ, et al. Subretinal delivery of adeno-associated virus serotype 2 results in minimal immune responses that allow repeat vector administration in immunocompetent mice. J Gene Med 2009;11:486–497.

56. Heavner W, Pevny L. Eye development and retinogenesis. Cold Spring Harb Perspect Biol 2012;4:a008391.

57. Haskell RE, Hughes SM, Chiorini JA, et al. Viral-mediated delivery of the late-infantile neuronal ceroid lipofuscinosis gene, TPP-I to the mouse central nervous system. Gene Ther 2003;10:34–42.

58. Passini MA, Dodge JC, Bu J, et al. Intracranial delivery of CLN2 reduces brain pathology in a mouse model of classical late infantile neuronal ceroid lipofuscinosis. J Neurosci 2006;26:1334–1342.

59. Sondhi D, Hackett NR, Peterson DA, et al. Enhanced survival of the LINCL mouse following *CLN2* gene transfer using the rh.10 rhesus macaque-derived adeno-associated virus vector. Mol Ther 2007;15:481–491.

60. Crystal RG, Sondhi D, Hackett NR, et al. Clinical protocol. Administration of a replication-deficient adeno-associated virus gene transfer vector expressing the human CLN2 cDNA to the brain of children with late infantile neuronal ceroid lipofuscinosis. Hum Gene Ther 2004;15:1131–1154.

61. Katz ML, Tecedor L, Chen Y, et al. AAV gene transfer delays disease onset in a TPP1-deficient canine model of the late infantile form of Batten disease. Sci Transl Med 2015;7:313ra180.

62. Griffey M, Macauley SL, Ogilvie JM, et al. AAV2-mediated ocular gene therapy for infantile neuronal ceroid lipofuscinosis. Mol Ther 2005;12:413–421.

63. Griffey MA, Wozniak D, Wong M, et al. CNS-directed AAV2-mediated gene therapy ameliorates functional deficits in a murine model of infantile neuronal ceroid lipofuscinosis. Mol Ther 2006;13:538–547.

64. Worgall S, Sondhi D, Hackett NR, et al. Treatment of late infantile neuronal ceroid lipofuscinosis by CNS administration of a serotype 2 adeno-associated virus expressing CLN2 cDNA. Hum Gene Ther 2008;19:463–474.

65. Chang M, Cooper JD, Sleat DE, et al. Intraventricular enzyme replacement improves disease phenotypes in a mouse model of late infantile neuronal ceroid lipofuscinosis. Mol Ther 2008;16:649–656.

66. Lu J-Y, Hu J, Hofmann SL. Human recombinant palmitoyl-protein thioesterase-1 (PPT1) for preclinical evaluation of enzyme replacement therapy for infantile neuronal ceroid lipofuscinosis. Mol Genet Metab 2010;99:374–378.

67. Griffey M, Bible E, Vogler C, et al. Adeno-associated virus 2-mediated gene therapy decreases autofluorescent storage material and increases brain mass in a murine model of infantile neuronal ceroid lipofuscinosis. Neurobiol Dis 2004;16:360–369.

68. Jakovcevski M, Guo Y, Su Q, et al. rAAV9—a human-derived adeno-associated virus vector for efficient transgene expression in mouse cingulate cortex. Cold Spring Harb Protoc 2010;4:pdb.prot5417.

69. Gray SJ, Nagabhushan Kalburgi S, McCow TJ, et al. Global CNS gene delivery and evasion of anti-AAV-neutralizing antibodies by intrathecal AAV administration in non-human primates. Gene Ther 2013;20:450–459.

70. Drack AV, Mullins RF, Pfeifer WL, et al. Immunosuppressive treatment for retinal degeneration in juvenile neuronal ceroid lipofuscinosis (juvenile Batten disease). Ophthalmic Genet 2015;36:359–364.

71. Seehafer SS, Ramirez-Montealegre D, Wong AM, et al. Immunosuppression alters disease severity in juvenile Batten disease mice. J Neuroimmunol 2011;230:169–172.

72. Simon DM, Levin S. Infectious complications of solid organ transplantations. Infect Dis Clin North Am 2001;15:521–549.

73. Kasiske BL, Snyder JJ, Gilbertson DT, et al. Cancer after kidney transplantation in the United States. Am J Transplant 2004;4:905–913.

74. Briggs JD. Causes of death after renal transplantation. Nephrol Dial Transplant 2001;16:1545–1549.

Received for publication April 22, 2016;
accepted after revision June 7, 2016.

Published online: July 11, 2016.